On Noise Correlation in Interference Alignment for MIMO Power Line Communications

Md Jahidur Rahman
Modem Technology Systems Group
Qualcomm Technologies, Inc.
San Diego, CA USA
E-mail: rahman@qti.qualcomm.com

Lutz Lampe
Dept. of Electrical and Computer Engineering
The University of British Columbia
Vancouver, BC Canada
Email: lampe@ece.ubc.ca

***Abstract*—The power line is inherently a broadcast medium when used for data transmission, since the electricity grid has no well defined boundaries for communication signals. This broadcast nature of the channel leads to mutual interference of communication signals emitted in relative proximity. To overcome the rate-limiting effect of this interference, recently the concept of interference alignment (IA) has been applied to power line communications (PLC). In particular, the benefits of IA have been shown for transmission in multi-input multi-output (MIMO) PLC systems. However, the results were obtained under the assumption of independent noise at the different ports of the PLC receiver. Unlike for most wireless communications scenarios for which IA has usually been studied, this assumption is often not valid for MIMO PLC. In particular, due to the dominance of noise signals induced and broadcast from grid-connected devices as well as the signal cross-coupling in PLC networks, noise is often found to be spatially correlated. Therefore, in this paper we explore the performance of IA for MIMO PLC in the presence of correlated noise obtained from indoor measurements. To this end, we adopt the maximum signal-to-interference-plus-noise ratio IA algorithm, whose formulation includes the noise statistics. Numerical results quantify the effect of noise correlation on the achievable sum-rate for MIMO PLC with IA.**

I. Introduction

Power line communication (PLC) reuses the power gird infrastructures for data communication. The main benefit of this approach is the high penetration of PLC signals without the need for extra wiring [1]. PLC has undergone tremendous innovations over the past two decades, often based on modern communication-theoretic concepts and inspired by their successful application in wireless and other communication systems over dedicated media [2]. One such innovation is the introduction of multi-input multi-output (MIMO) transmission over PLC networks [3], [4]. The underlying premise is the availability of three or more conductors, typically phase (P), neutral (N) and earth (E) wires, over which two or more signals can be transmitted in parallel. MIMO PLC has now become part of PLC standards and products [4].

PLC signals travel along the power line channel in a broadcast fashion without well defined boundaries. As it is illustrated in Fig. 1, the data transmission from a transmitter (Tx1) to an intended receiver (Rx1) will also broadcast to and thus interfere signal reception at other receivers (Rx2 and Rx3) in the network. Hence, multiple connections sharing the common power line medium experience an interference channel. For

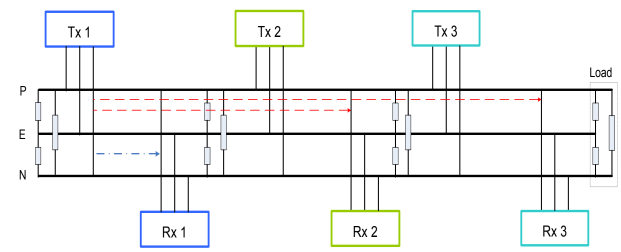

Fig. 1. Illustration of a 3-conductor-cable MIMO PLC network with three Tx-Rx pairs, communicating as an interference network. The broadcast nature of signal transmission (denoted by dash-dotted line) to an intended receiver causes interference (denoted by dashed lines) to other receivers in the network. The impedances represent different electrical loads (e.g., electrical appliances) connected to the power lines in indoor applications.

such a scenario, the application of interference alignment (IA) has been shown to increase the available degrees-of-freedom in the network [5], [6], [7]. This has often been applied and exploited for wireless communication systems and recently also for PLC. In particular, linear IA has been investigated and shown to improve the sum-rate in MIMO PLC networks [8]. The results in [8] also indicate some performance differences to IA in wireless communications owing to the specifics of shared PLC channels. One shortcoming of the initial work in [8] was the assumption of additive white Gaussian noise (AGWN) independent at the different receiver ports. Since noise in PLC is dominated by disturbances induced into the grid from attached appliances and equipments, it is generally spectrally and spatially not white. This has been substantiated in various measurement campaigns for MIMO PLC in indoor environments [9]–[12]. While spectral dependencies are of somewhat secondary importance for the operation of linear IA over spatial MIMO channel, the spatial correlation is directly relevant for the IA filter design and performance.

Concerning this, in this paper we investigate the impact of spatial noise correlation on the performance of linear IA for MIMO PLC. We exploit the practical noise data collected by the special task force 410 (STF-410) of the European Telecommunication Standardization Institute (ETSI) during a measurement campaign in several homes throughout Europe

[11],[12]. The availability of the measured noise data allows us to evaluate the IA performance with practical levels of spatial noise correlation in real MIMO PLC networks. Since the results in [8] suggest that the maximum signal-to-interference-plus-noise ratio (Max-SINR) based IA design provides a better sum-rate performance than the minimum interference leakage (Min-IL) based design and also has the ability to take into account the noise statistics [13], we adopt the former for our studies. Our specific objectives are twofold. First, we examine the impact of spatially correlated noise on performance when the Max-SINR is designed assuming independent noise across different ports, which could be considered as a mismatched design. This is to say, we investigate the benefits of incorporating noise correlation into the IA design. Second, we show that assuming spatially independent noise at different PLC receiver ports underestimates achievable rates. Overall, our results highlight that proper exploitation of practical noise correlation levels in PLC leads to further gains in sum-rate for transmission with IA. More specifically, with a proper IA design that accounts for practical noise correlation levels, a rate gain as high as 34% over a mismatched IA design is obtained for the considered PLC setup.

The rest of the paper is organized as follows. Section II describes the system model for a MIMO PLC network, including precoding, receive signal processing, and the Max-SINR IA algorithm. The processing of the measured noise, along with the numerical results are discussed in Section III. Finally, the paper is summarized in Section IV.

II. System Model

We consider an $(N+1)$-conductor MIMO PLC network, where there are K transmitter-receiver (Tx-Rx) pairs, as illustrated in Fig. 1 for $N = 2$ and $K = 3$. Each Tx-Rx pair is able to make use of N feeding and receiving ports at the corresponding transmitter and receiver, respectively. We assume that all transmitters communicate simultaneously to their unique intended receiver, thereby creating an interference-limited communication scenario, alike the more commonly considered wireless interference channel scenario.

We assume broadband transmission for high-rate (indoor) PLC communications, which is typically based on orthogonal frequency-division multiplexing (OFDM) [1], [2]. We thus can restrict ourselves to the description of IA for one OFDM subcarrier in the frequency domain in the following, and consider the full broadband OFDM system for the numerical results in Section III.

A. Precoding at the PLC Transmitter

Each transmitter, $i = 1, \ldots, K$, sends $d_i \leq N$ independent data streams, x_i^m, $m = 1, \ldots, d_i$. The data stream is assigned a power p_i^m such that $\sum_{m=1}^{d_i} p_i^m \leq P_i$, where P_i is the maximum power of transmitter i. The message x_i^m is sent along the beamforming vector $v_i^m \in \mathbb{C}^N$, so that the overall transmit symbol $s_i \in \mathbb{C}^N$ reads

$$s_i = \sum_{m=1}^{d_i} v_i^m x_i^m = V_i x_i \ , \tag{1}$$

where $V_i = [v_i^1, v_i^2, \ldots, v_i^{d_i}] \in \mathbb{C}^{N \times d_i}$ and $x_i = [x_i^1, \ldots, x_i^{d_i}]^T \in \mathbb{C}^{d_i}$. This precoding requires channel state information (CSI) at the transmitter. This can be assumed for broadband PLC, where transmitter side CSI is also used for bit-loading.

B. The PLC Channel

The received signal $r_i \in \mathbb{C}^N$ at PLC receiver i is given by

$$r_i = H_{i,i} s_i + \sum_{j=1, j \neq i}^{K} H_{i,j} s_j + n_i \ , \tag{2}$$

where $H_{i,j} \in \mathbb{C}^{N \times N}$ is the matrix of samples of the channel frequency responses for the considered subcarrier between transmitter j and receiver i and $n_i \in \mathbb{C}^N$ is the vector of frequency-domain noise samples at the different ports of PLC receiver i. We can assume that n_i is Gaussian distributed with the covariance matrix Ψ_i,

$$\Psi_i = \begin{bmatrix} \psi_{ii} & \psi_{ij} \\ \psi_{ji} & \psi_{jj} \end{bmatrix} , \tag{3}$$

whose off-diagonal elements are non-zero for spatially correlated receiving ports [9]–[12]. We note that PLC noise may also contain a non-stationary impulse component, whose presence is however not primarily important for the study of IA transmission, as the occurrence of impulses would typically lead to outages similar to the case of non-IA transmission.

C. Processing at the PLC Receiver

The received signal is projected onto the columns of a receive filter, $U_i = [u_i^1, \ldots, u_i^{d_i}] \in \mathbb{C}^{N \times d_i}$. The received signal for the mth stream is then recovered as

$$\begin{aligned} y_i^m &= (u_i^m)^{\mathrm{H}} r_i \qquad (4) \\ &= (u_i^m)^{\mathrm{H}} H_{i,i} v_i^m x_i^m + (u_i^m)^{\mathrm{H}} \sum_{(j,l) \neq (i,m)} H_{i,j} v_j^l x_j^l + (u_i^m)^{\mathrm{H}} n_i, \qquad (5) \end{aligned}$$

where $(\cdot)^{\mathrm{H}}$ denotes the Hermitian transpose operation. The corresponding SINR follows as

$$\Gamma_i^m = \frac{p_i^m \| (u_i^m)^{\mathrm{H}} H_{i,i} v_i^m \|_2^2}{(u_i^m)^{\mathrm{H}} \Phi_i^m (u_i^m)} , \tag{6}$$

where $\| \cdot \|_2$ denotes ℓ_2-norm and the corresponding interference-plus-noise covariance matrix is defined as

$$\Phi_i^m = \sum_{(j,l) \neq (i,m)} p_j^l H_{i,j} v_j^l (v_j^l)^{\mathrm{H}} H_{i,j}^{\mathrm{H}} + \Psi_i \ . \tag{7}$$

D. The IA Algorithm

As mentioned earlier, the precoding and projection filters are obtained by the Max-SINR algorithm. For given precoding filters, the receiver filters are obtained from [13]

$$\hat{u}_i^m = \arg\max_{u_i^m} \Gamma_i^m \tag{8}$$

as

$$\hat{u}_i^m = \frac{(\Phi_i^m)^{-1} H_{i,i} v_i^m}{\|(\Phi_i^m)^{-1} H_{i,i} v_i^m\|_2} \,. \tag{9}$$

The precoding filters are then designed via exchanging the roles of transmitters and receivers [13]. We note that (9) accounts for the noise correlation. The orthogonalized output precoding and projection filters are then scaled to satisfy the power constraint, P_i, $\forall i$ [14].

III. Numerical Results and Discussions

To quantify the performance of the Max-SINR based IA design in the presence of spatially correlated noise, we simulate an interference-limited MIMO PLC network as it is illustrated in Fig. 1 for $K = 3$ and $N = 2$. We set the distance between each Tx-Rx pair at 100 and 200 meters to simulate two different network scenarios, i.e., network scenarios 1 and 2, respectively. The shorter distance between the Tx-RX pairs may replicate a power line wiring in a house, while the larger distance replicates the same in a large office. In both network scenarios, PLC transmitters and receivers are terminated with load resistances chosen from the range between 10Ω to 50Ω. We consider the frequency band from 2 to 30 MHz and calculate channel frequency responses between different Tx-Rx pairs at a frequency separation of 24.4 kHz. This imitates the use of OFDM as typical for broadband PLC systems. The computation of the channel frequency response is based on multiconductor transmission-line theory [15], and obtained via the emulator reported in [16]. For the PLC MIMO transmission, we consider two configurations: transmission using the P-E/N-E and the P-N/N-E ports, respectively. The total transmit power spectral density (PSD) over both ports is set to -55 dBm/Hz, which is a commonly applied spectral mask for broadband PLC systems [4].

The additive noise is taken from measured noise traces made available to us and reported in [11], [12]. Since the measurement probe applied a star-style receiver [11], [12] while we consider a delta-type receiver (see Fig. 1, cf. [4, Ch. 1]), we take the difference of time domain measured noise between ports P, E, and N, to obtain equivalent noise in delta-type receiver configuration. We denote such possible modes as P-N, P-E, and N-E. We then obtain the noise covariance matrix of the noise through the use of Welch's spectral estimation technique. We assume that each transmitter sends a single data stream, i.e., $d_i = 1$, $\forall i$, and that $P_i = P$, $\forall i$, according to the above-mentioned PSD limit. Then the achievable sum-rate for a given subcarrier with IA transmission and correlated noise can be derived as

$$R = \sum_{i=1}^{K} \log_2 \left(1 + \frac{S_i S_i^{\mathrm{H}}}{J_i (J_i)^{\mathrm{H}} + U_i^{\mathrm{H}} \Psi_i U_i}\right), \tag{10}$$

where $S_i \triangleq \sqrt{P} U_i^{\mathrm{H}} H_{i,i} V_i$ and $J_i \triangleq \sqrt{P} U_i^{\mathrm{H}} \sum_{k \neq i} H_{i,k} V_k$.

We now investigate the rate performances for two IA designs: one that incorporates the noise correlation, i.e., a proper design and one that assumes uncorrelated noise in the IA filter computation (9), thus rendering a mismatched design. The latter can be considered as a benchmark design, for the case that an estimation of the noise correlation is not attempted. We first evaluate the performances of these designs for a noise dataset collected in Valencia, Spain (henceforth, denoted as dataset 1) at three different outlets (OLs) in the frequency range $2-30$ MHz [11], [12]. While receiving ports may have roughly similar noise PSDs, the spatial correlations across these ports can be substantially different. For example, the average noise PSDs of the P-E and N-E receiving ports at OL 3 are about -67 dBm/Hz, while the spatial correlations across P-E/N-E and P-N/N-E receiving ports are 0.56 and 0.28, respectively.

Figs. 2 and 3 illustrate the rate gains of the matched (proper) IA design over the mismatched one as a function of the subcarrier index using the measured noise at OL 3 and network scenario 2 across P-E/N-E and P-N/N-E ports, respectively. We notice that considering actual noise correlation in the IA design leads to significant improvements in the rate performances. For example, the improvement for transmission over P-E/N-E ports, as shown in Fig. 2, can be as high as 390% for individual subcarriers and it is 34% on average. We also observe that the (average) sum-rate gain is substantially larger for the port

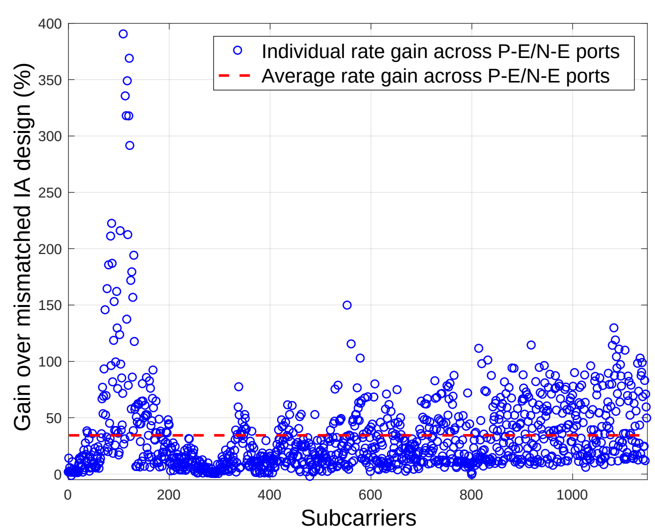

Fig. 2. Subcarrier rate gain for a matched IA design with correlated noise over a mismatched IA design (i.e., that ignores spatial noise correlation during IA filter computation) for OL 3 of the dataset 1 across P-E/N-E ports in the network scenario 2.

TABLE I
RATE GAIN OF THE MATCHED OVER THE MISMATCHED IA DESIGN FOR DIFFERENT NOISE DATA SETS AND PLC MIMO CONFIGURATIONS.

		Network Scenario 1		Network Scenario 2	
Noise Datasets	Outlets	Avg. Gain (P-E/N-E)	Avg. Gain (P-N/N-E)	Avg. Gain (P-E/N-E)	Avg. Gain (P-N/N-E)
1	1	16.92%	10.90%	28.17%	16.48%
	2	14.88%	5.23%	31.19%	8.96%
	3	16.80%	8.05%	34.38%	12.66%
2	1	6.64%	5.49%	19.17%	15.78%
	2	11.93%	6.22%	30.33%	15.75%

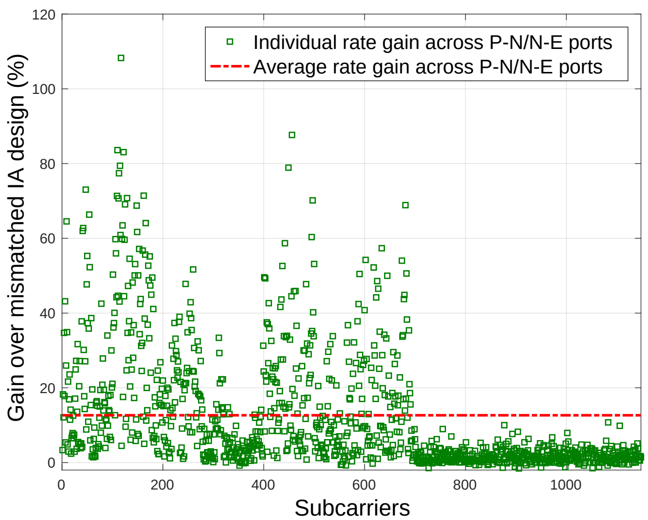

Fig. 3. Subcarrier rate gain for a matched IA design with correlated noise over a mismatched IA design across P-N/N-E ports with the same network configuration as in Fig. 2.

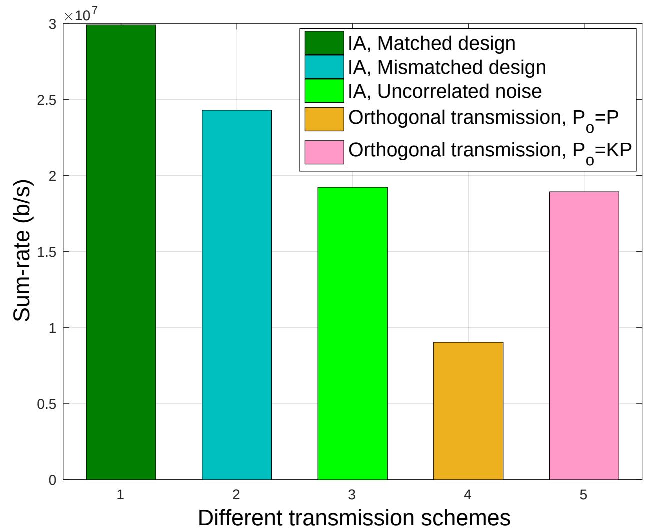

Fig. 4. Comparison of sum-rate performances among different IA designs and orthogonal transmissions for OL 3 across P-E/N-E ports of the dataset 1 in the network scenario 2.

configuration with the large noise correlation. This is not only due to a more pronounced receiver mismatch but also due to fact that noise correlation generally improves the achievable rate. Finally, we note that for few subcarriers the rate gain is negative, i.e., the mismatched IA design assuming uncorrelated noise performs better than the matched design. We attribute this to the fact that the Max-SINR algorithm may be stuck in a local optimum as convergence to the global optimum point is not guaranteed due to the non-convex nature of the optimization problem [13].

Table I summarizes the rate gain results for noise data collected at the OLs for two different locations. Here, we also provide the results for a noise dataset from Paiporta, Spain (henceforth, denoted as dataset 2) at two different OLs. The noise in this location has a relatively lower average PSD than that of the dataset 1 (e.g., at OL 2, the average noise PSDs of P-E and N-E receiving ports are about -75 dBm/Hz). Hence, the signal to noise ratio (SNR) is relatively higher than for the dataset 1. While the average correlation coefficient across P-E/N-E ports at this OL is 0.53 and thus similar to that in OL 3 of the dataset 1, the average correlation coefficient across the P-N/N-E ports is significantly higher at 0.37. We observe that notable rate gains are achieved for all test cases. Although, they are relatively lower for the higher SNR case, e.g., network scenario 1 vs. network scenario 2 due to short transmission distances for the former, and OL 3 of the dataset 1 vs. OL 1 of the dataset 2 due to lower noise PSD for the latter. Owing to the higher correlation across P-N/N-E ports for the dataset 2, however, the rate gains for these ports are comparable in the network scenario 2 despite having lower noise PSD. A similar explanation holds across P-E/N-E ports, e.g., for OL 2 of the dataset 2 when compared with OL 1 of the dataset 1 in the network scenario 2.

We finally compare the system sum-rate performances for the network scenario 2 considering correlated noise from the dataset 1 at OL 3 for (1) a matched and (2) a mismatched IA design, as well as (3) an IA design assuming uncorrelated noise with the same noise PSDs at the individual ports, i.e., the case that spatial noise correlation is absent. Fig. 4 shows the corresponding system sum-rate results. As a baseline, we also provide results with conventional orthogonal transmission, such as time division multiple access. While in one instance, labelled as case (4), we assume a transmit power, $P_\text{o} = P_i = P, \forall i$, for orthogonal transmission, we also simulate the case (5) where $P_\mathrm{o} = KP$, i.e., the system transmit power is identical to that in IA where all K users transmit simultaneously. Comparing cases (1) and (3) we observe that a channel with noise correlation supports a notably increased rate and that the matched IA design is able to reap those rate gains. Furthermore, comparing cases (1) to both (4) and (5), we conclude that the Max-SINR based IA design outperforms conventional channel orthogonalization technique in terms of system sum-rate, even if the latter was allowed to transmit with a much higher per-user transmit power.

IV. Conclusions

In this paper, we have investigated the performance of the Max-SINR based IA design with measured MIMO PLC noise, where the noise is spectrally colored and spatially correlated. Our results quantify the performance gain that can be achieved through a proper IA design that accounts for spatial noise correlation. In particular, while noise correlations are generally beneficial in that they allow for improved transmission rates, our results show for realistic PLC sample cases that rate gains of e.g., 34% are realized when linear IA includes the spatial correlation in the filter design.

V. Acknowledgement

The authors would like to thank Dr. Andreas Schwager from Sony, Europe for providing us access to the measured noise data for MIMO PLC. This work was supported in part by the Natural Sciences and Engineering Research Council of Canada (NSERC)

References

[1] L. Lampe, A. Tonello, and T. Swart, Eds., *Power Line Communications: Principles, Standards and Applications from Multimedia to Smart Grid*, 2nd ed. UK: John Wiley & Sons Ltd, Jun. 2016.

[2] C. Cano, A. Pittolo, D. Malone, L. Lampe, A. M. Tonello, and A. G. Dabak, "State of the art in power line communications: From the applications to the medium," *IEEE J. Sel. Areas Commun.*, vol. 34, no. 7, pp. 1935–1952, Jul. 2016.

[3] D. Schneider, J. Speidel, L. Stadelmeier, and D. Schill, "Precoded spatial multiplexing MIMO for inhome power line communications," in *IEEE Global Communications Conference*, pp. 1–5, Nov. 2008.

[4] L. T. Berger, A. Schwager, P. Pagani, and D. M. Schneider, Eds., *MIMO Power Line Communications: Narrow and Broadband Standards, EMC, and Advanced Processing*. New York, NY: CRC Press - Taylor & Francis Group, 2014.

[5] M. A. Maddah-Ali, A. S. Motahari, and A. K. Khandani, "Communication over MIMO X channels: Interference alignment, decomposition, and performance analysis," *IEEE Trans. Inf. Theory*, vol. 54, no. 8, pp. 3457–3470, Aug. 2008.

[6] V. R. Cadambe and S. A. Jafar, "Interference alignment and degrees of freedom of the K-user interference channel," *IEEE Trans. Inf. Theory*, vol. 54, no. 8, pp. 3425–3441, Aug. 2008.

[7] S. A. Jafar, "Interference alignment–a new look at signal dimensions in a communication network," *Foundations and Trends in Communications and Information Theory*, vol. 7, no. 1, pp. 1–134, 2011. [Online]. Available: http://dx.doi.org/10.1561/0100000047

[8] Md. J. Rahman and L. Lampe, "Interference alignment for MIMO power line communications," in *IEEE Intl. Symp. Power Line Communications and Its Applications (ISPLC)*, pp. 71–76, Mar. 2015.

[9] D. Rende, A. Nayagam, K. Afkhamie, L. Yonge, R. Riva, D. Veronesi, F. Osnato, and P. Bisaglia, "Noise correlation and its effect on capacity of inhome MIMO power line channels," in *IEEE Intl. Symp. Power Line Communications and Its Applications (ISPLC)*, pp. 60–65, Apr. 2011.

[10] A. Pittolo, A. M. Tonello, and F. Versolatto, "Performance of MIMO PLC in measured channels affected by correlated noise," in *IEEE Intl. Symp. Power Line Communications and Its Applications (ISPLC)*, pp. 261–265, Mar. 2014.

[11] A. Schwager, W. Bschlin, H. Hirsch, P. Pagani, N. Weling, J. L. G. Moreno, and H. Milleret, "European MIMO PLT field measurements: Overview of the ETSI STF410 campaign and EMI analysis," in *IEEE Intl. Symp. Power Line Communications and Its Applications (ISPLC)*, pp. 298–303, Mar. 2012.

[12] "Setup and statistical results of MIMO PLT channel and noise measurements," *ETSI TR 101 562-3 V1.1.1*, 2012.

[13] K. Gomadam, V. R. Cadambe, and S. A. Jafar, "A distributed numerical approach to interference alignment and applications to wireless interference networks," *IEEE Trans. Inf. Theory*, vol. 57, no. 6, pp. 3309–3322, Jun. 2011.

[14] D. S. Papailiopoulos and A. G. Dimakis, "Interference alignment as a rank constrained rank minimization," *IEEE Trans. Signal Process.*, vol. 60, no. 8, pp. 4278–4288, Aug. 2012.

[15] F. Versolatto and A. Tonello, "An MTL theory approach for the simulation of MIMO power-line communication channels," *IEEE Trans. Power Del.*, vol. 26, no. 3, pp. 1710–1717, Jul. 2011.

[16] F. Gruber and L. Lampe, "On PLC channel emulation via transmission line theory," in *IEEE Intl. Symp. Power Line Communications and Its Applications (ISPLC)*, pp. 178–183, Mar. 2015.